

# Formation of metre-scale bladed roughness on Europa's surface by ablation of ice

Daniel E. J. Hobley<sup>1\*</sup>, Jeffrey M. Moore<sup>2</sup>, Alan D. Howard<sup>3</sup> and Orkan M. Umurhan<sup>2</sup>

**On Earth, the sublimation of massive ice deposits at equatorial latitudes under cold and dry conditions in the absence of any liquid melt leads to the formation of spiked and bladed textures eroded into the surface of the ice. These sublimation-sculpted blades are known as penitentes. For this process to take place on another planet, the ice must be sufficiently volatile to sublimate under surface conditions and diffusive processes that act to smooth the topography must operate more slowly. Here we calculate sublimation rates of water ice across the surface of Jupiter's moon Europa. We find that surface sublimation rates exceed those of erosion by space weathering processes in Europa's equatorial belt (latitudes below 23°), and that conditions would favour penitente growth. We estimate that penitentes on Europa could reach 15 m in depth with a spacing of 7.5 m near the equator, on average, if they were to have developed across the interval permitted by Europa's mean surface age. Although available images of Europa have insufficient resolution to detect surface roughness at the multi-metre scale, radar and thermal data are consistent with our interpretation. We suggest that penitentes could pose a hazard to a future lander on Europa.**

The Jovian moon of Europa hosts an interior ocean of liquid water<sup>1–3</sup>, and has been proposed as a target for future planetary missions due to the possible habitability of this ocean. Past studies of its icy shell have envisioned a surface that is smooth at the lander scale, dominated by diffusive impact processes such as impact gardening and sputtering by charged particles in Jupiter's magnetic field<sup>4–10</sup>. However, on Earth, icy surfaces ablated by solar radiation develop characteristic roughness patterns at the centimetre to multi-metre scale<sup>11–16</sup>. Here we show that under modern Europan conditions, sublimation processes driven by solar radiation flux are expected to dominate over diffusive processes in a band around the satellite's equator. As the surface at these latitudes degrades, it will develop an east-west aligned, spiked and bladed texture, or roughness, at the metre scale – known on Earth as penitentes. This interpretation can explain anomalous radar returns seen around Europa's equator<sup>4,5,17</sup>. Penitentes may well explain reduced thermal inertias and positive circular polarization ratios in reflected light from Europa's equatorial region<sup>17,18</sup>. This formation mechanism is used to explain formation of bladed terrain on Pluto in methane ice<sup>19</sup>.

## Blade formation by sublimation

Self-organized surface patterning is ubiquitous in terrestrial snow and ice during ablation by radiative heating, through both sublimation and melting. Europa's atmosphere is so tenuous ( $\sim 0.1 \mu\text{Pa}$ ,  $10^{12}$  times less than Earth's surface; 10–20 km particle mean free paths<sup>20</sup>) that its external heat budget is effectively radiative, and hence such textures might also be expected there on ablating surfaces, but solely due to sublimation. On Earth, growth of these patterns is linked to amplification of initial random depressions in the surface by lensing of scattered solar and thermal infrared radiation<sup>11,16,21</sup>.

On Earth, the dominant radiative structures that form in snow and ice under cold, dry conditions are called penitentes. These are tall, east-west aligned, sharp-edged blades and spikes of sculpted snow or ice which point towards the elevation of the midday sun<sup>12,22</sup> (Fig. 1). Typical heights are 1–5 m. Formation of large and

well-developed penitentes requires bright, sustained sunlight, cold, dry, still air<sup>11</sup>, and a melt-free environment<sup>12</sup>. Thus, they are almost entirely restricted to high-altitude tropics and subtropics<sup>14</sup>. Laboratory experiments<sup>22</sup> and numerical modelling<sup>16</sup> confirm that sublimation in the absence of melting is particularly essential for penitente formation<sup>11,12</sup>. Small amounts of dirt in the ice do not inhibit penitente formation if radiation can penetrate the ice, and the vapour can escape<sup>11,16,22</sup>.

Radiative modelling confirms that penitentes form by scattering and lensing of light on and into snow and ice<sup>11,16</sup>. A key factor controlling penitente formation is that the pit of the structure must ablate faster than the sidewalls; if the sidewalls ablate faster, an alternate bowl-like stable form known as a suncup may develop<sup>13,15,16</sup>. Penitente growth requires a daily low solar incidence angle, such that light strikes the walls of the blades at a high angle, and illuminates the floors of the pits<sup>13,14</sup>. This maximizes the contrast in flux per unit area on the floor compared to the sidewalls, both in terms of direct and scattered radiation<sup>14</sup>, and explains why terrestrial examples are usually found near the equator, or also on steep equatorward-facing slopes at higher latitudes<sup>23</sup>. Physical analysis indicates that the scale and stability of penitentes are critically controlled by the thermal absorption of solar radiation into the ice and by the ability of the system to sustain gradients in the vapour pressure of the atmosphere that is in contact with the ice<sup>16</sup>. Theory suggests that the minimum size of penitentes may be governed by any of the following physical parameters: light extinction depth<sup>11,22</sup>, atmospheric vapour diffusion<sup>16</sup>, or heat conduction<sup>16</sup>. Their growth is most rapid for penitentes of sizes close to this minimum scale. This implies that ice grain size, porosity, roughness and impurity concentrations affect penitente size. Experiments, however, suggest that penitente size increases with depth of incision, and that a characteristic depth-to-width (aspect) ratio of about 2 is obtained, similar to 1.5–1.7 in terrestrial penitente fields<sup>13</sup>. The focusing of radiation in shallow hollows means that they will deepen, but shadowing and multiple reflections limit the depth of penitentes<sup>23,24</sup>, implying an optimum aspect ratio. Whether penitentes grow in size without limit during

<sup>1</sup>School of Earth & Ocean Sciences, Cardiff University, Cardiff, UK. <sup>2</sup>NASA Ames Research Center, Moffett Field, CA, USA. <sup>3</sup>Dept. Environmental Sciences, University of Virginia, Charlottesville, VA, USA. \*e-mail: [HobleyD@cardiff.ac.uk](mailto:HobleyD@cardiff.ac.uk)



**Fig. 1 | Terrestrial penitentes from the southern end of the Chajnantor plain, Chile.** The view is broadly northwards; blades can be seen perpendicular to the viewing direction. The extreme relief of the structures is typical. The depressions between these examples have ablated down to the underlying rock surface. Credit: ESO ([https://www.eso.org/public/images/img\\_1824/](https://www.eso.org/public/images/img_1824/)).

continued sublimation is uncertain, but eventually the mechanical strength of  $\text{H}_2\text{O}$  ice will limit the size.

These observations suggest that sublimation on Europa could create penitente-like textures on its surface. Europa is tidally locked to Jupiter, with an inclination to Jupiter's equator of  $0.47^\circ$ . Jupiter's obliquity is only  $3.13^\circ$ , and thus for any given point on Europa's surface, the solar zenith angle never varies by  $>4^\circ$ . This orbital configuration has likely been stable over the lifetime of the surface<sup>25</sup>. Based on Galileo Photopolarimeter-Radiometer (PPR) data, surface brightness temperatures have been calculated to vary between  $\sim 70\text{ K}$  and  $132\text{ K}$ <sup>4,5</sup>. Its photometric properties, in particular its albedo, show that the surface of Europa is fairly pure water ice, with a minor component of silicate materials and salts<sup>2,5,7</sup>. Thus, the surface fulfills three essential requirements for penitente growth - it is dominantly exposed ice; it would sublime without melting; and there is very little variation in solar incidence angle.

Furthermore, for penitentes to develop, they must grow faster than any other geomorphic process can modify the surface. Europa is subjected to bombardment both by conventional impactors (meteoroids, comets) and by ions accelerated by Jupiter's magnetic field<sup>5,26,27</sup>. Both of these processes will act diffusively to smooth out local topographic highs. The most recent estimates<sup>5,8,9</sup> suggest that ion sputtering is probably dominant over impact gardening on Europa today, with rates of  $\sim 2 \times 10^{-2}\text{ m Ma}^{-1}$ . At first order, for penitentes to develop, the sublimation rate must minimally exceed these diffusive processes. We assess sublimation rates using global maps of peak brightness temperatures coupled to profiles of temperature variation throughout the day<sup>4,5</sup> to input into temperature-dependent equations of state (see Methods). This allows us to predict the approximate rates of uniform sublimation at varying Europaan latitudes (Fig. 2). Bulk surface sublimation rates exceed likely sputtering erosion rates equatorwards of latitudes  $24^\circ\text{ N/S}$  ( $\pm 6^\circ$ ), dependent on the modelling assumptions. We hypothesize that penitentes can grow, and indeed have grown, in this region.

Studies of terrestrial development of penitentes provide support for order-of-magnitude estimates of the dimensions of these structures, at least with respect to their aspect ratios. On Earth, the rate of growth as well as the characteristic separation scale of the ice blades is modelled to be set by the balance between heat conductivity in the ice, mass diffusion, and bolometric albedo<sup>16</sup>. On Earth the mass diffusion term is, in turn, set by an atmospheric boundary layer thickness.

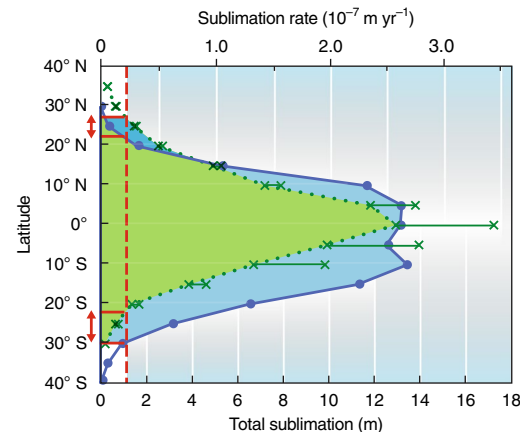


**Fig. 2 | Modelled variation in rates of surface sublimation, and equivalent total depth of ice removal, with Europaan latitude.** Latitudinally dependent sublimation rates (top axis) and corresponding total sublimated ice over a  $50\text{ Ma}$  timescale (bottom axis) are derived from distinct brightness temperature data sets from two Galileo orbits, G7 (blue circles, solid line) and I25 (green crosses, dotted line), each of which are centered on opposite hemispheres. Due to truncated observations, both maxima and minima are shown for orbit I25. Temperatures are estimated based on an emissivity value of 0.90 (see Methods). Green and blue shaded regions indicate conservative rate estimates for the two data sets. Red dashes show average rates of surface overturn by sputtering. Red arrows indicate the latitudinal range in which predicted sublimation rates, based on G7 and I25 orbit observations, equal the overturn rate driven by sputtering. In both hemispheres, sublimation outcompetes sputtering erosion in a broad equatorial band equatorwards of  $\sim \pm 24^\circ$  latitude, and it is this surface that could develop penitentes.

This does not apply to Europa, however, due to its insignificant atmosphere ( $\sim 10^{-8}\text{ Pa}$ ). For Europa, we first estimate the rate of ice sublimation at the equator, finding approximately  $0.3\text{ m Ma}^{-1}$  (see Methods). Based on this analysis we infer that sublimation outpaces sputtering and impact gardening by an order of magnitude.

Based upon our analysis, up to  $15\text{ m}$  of sublimation has occurred over  $50\text{ Ma}$ , which is the average surface age of Europa<sup>5,8</sup>. We next assume that penitentes grow with constant aspect ratio, which we assume to be  $\sim 2:1$ . Thus we conclude that maximum penitente depth could reach  $\sim 15\text{ m}$  with spacing of  $\sim 7.5\text{ m}$  near the equator (Fig. 2). We infer that the penitentes will become shallower, less well developed and increasingly asymmetric (and thus mechanically unstable) with distance from the equator<sup>23</sup> (see Methods).

Our sublimation calculations are zonally averaged, and do not account for a number of local or poorly constrained effects. For example, fissured, ridged, and chaotic textures seen at  $>0.1\text{ km}$  scales indicate that resurfacing occurs in different places at different times<sup>1,26</sup>. Young areas will clearly lack major penitentes, and older areas should have better developed structures. Local surface inclination will also alter growth rates and stability. We have not accounted for spatial variation in sputtering rates, particularly with respect to their leading-trailing hemispheric asymmetry<sup>27,28</sup>. We also cannot quantify the role of particulate impurity within and on the ice, and so this is not treated here<sup>6,7</sup>. Magnitudes of local relief and surface non-volatile contamination at Europa are badly constrained, especially at the key metre scales, but are likely variable and might be locally substantial<sup>29</sup>. Contamination can produce both positive and negative feedbacks<sup>11,22</sup>, and locally suppress penitente growth entirely if a substantial non-volatile surface lag has formed<sup>11,15</sup>. Re-deposition of sublimated ice will occur at high latitudes, polar-facing slopes, and local cold-traps<sup>5,6</sup>.

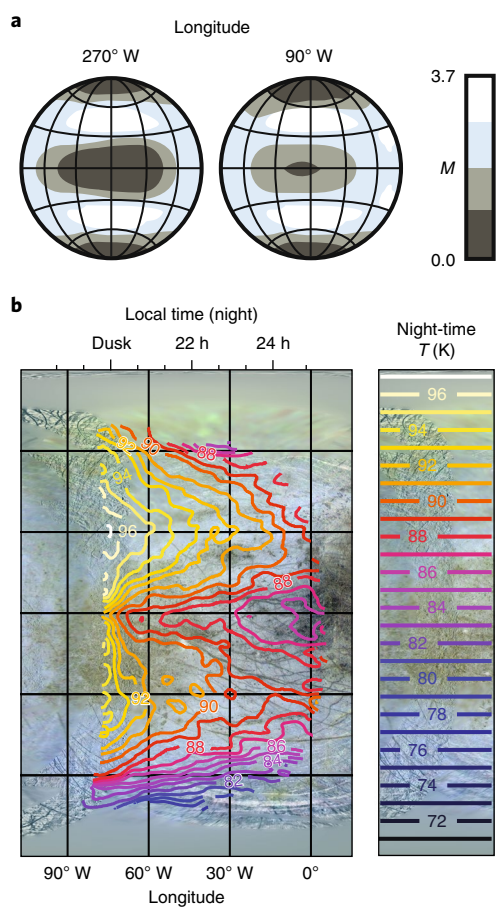


**Fig. 3 | Remote sensing evidence consistent with an equatorial band of penitentes on Europa.** **a**, Instantaneous total power radar albedo,  $M$ , returned from a 12.6 cm radar sounding of Europa using the Arecibo telescope. **b**, Instantaneous night-time brightness temperatures from the E17 orbital pass of Europa as inferred from Galileo PPR data (wavelength range 0.35–100  $\mu\text{m}$ ). Local time (top axis) is presented in Europa equivalent hours of the day. The instantaneous acquisition of the PPR data used here causes much of the surface viewed by that instrument to be seen at an oblique angle. The base map, from Galileo and Voyager images, is in a cylindrical projection and gridded at 30° of latitude and longitude. Panel **a** produced using data presented in Ostro et al.<sup>17</sup>, AGU. Panel **b** produced and modified using data presented in Rathbun et al.<sup>31</sup>, Elsevier; base map courtesy of P. Schenk/NASA.

### Supporting observations

Given our estimates of penitente spacing ( $\leq 7.5$  m), available imaging from the Galileo Orbiter's camera is too coarse to permit detection. Current roughness estimates are either at scales too coarse ( $> 10^1$  m, from imaging<sup>30</sup>) or too fine ( $< 10^{-2}$  m, from optical photometry<sup>10</sup>). Two independent and largely unexplained sets of ground-based radar and Galileo Orbiter thermal observations reveal, however, that the surface properties of Europa equatorwards of  $\sim \pm 25^\circ$  are systematically different to those polewards of those latitudes:

- (1) Instantaneous disk resolved radar returns from Europa reveal a striking equatorial minimum in the total power returned at 13 cm wavelengths<sup>17</sup> (Fig. 3a).
- (2) Maps of Europa's night-time brightness temperatures from Galileo's PPR instrument reveal a very similar equatorial minimum<sup>4,5</sup> (Fig. 3b). Previous authors have interpreted such brightness temperatures as indicating a relative minimum in surface thermal inertia at the equator<sup>4,31</sup>.

The known geology and visible surface patterning of Europa do not systematically change at the equator<sup>4,5</sup>, and this has made the above observations enigmatic. However, a penitente-like, ordered surface roughness, or texture, provides a possible solution. Because light entering a penitente hollow will, on average, interact more than once with the walls before emerging, the development of ice blades in these latitudes would increase the flat-surface-equivalent absorption coefficient, even with no change to fine scale material properties. In other words, the form of such a surface makes it an effective absorber for wavelengths shorter than the scale of the structure. By Kirchhoff's law, this also means that such a surface will be a more effective emitter, compared to an equivalent flat surface.

Further support comes from the leading/trailing hemispheric asymmetry in radar albedo of the equatorial regions. The trailing hemisphere ( $270^\circ$  W) is much more heavily contaminated with particulates transported there by the magnetosphere. The trailing hemisphere, however, has a higher equatorial radar albedo than the leading hemisphere (Fig. 3a). This is counterintuitive if the contaminants aid absorption of radar in the subsurface, but fits if high particulate concentrations partially suppress penitente formation.

Europa radar observations reveal atypical circular polarization ratios. This atypical pattern may also result from the presence of penitente fields. Earth-based whole-disc radar observations at wavelengths  $\lambda = 12.6$  cm reveal that unlike all known rocky bodies, the ratio of same-sense to opposite-sense circularly polarized radar,  $\mu_c$ , exceeds 1.0 for Europa, that is, the typical ray strikes an even number of surfaces before being detected<sup>17,18</sup>. Traditional explanations for this 'startling'<sup>18</sup> effect have relied on arbitrary, complex subsurface geometries—either randomly orientated ice dykes and fractures<sup>32</sup>, or buried, ideally-shaped impact craters<sup>33</sup>. However, a bladed surface texture at the surface could easily fulfill such a role, with the steeply inclined, opposing walls of the blades replacing the fractures or buried crater walls<sup>34</sup>. In incident radar at decimetre scales, the equator appears to be an anomalously effective absorber, hence the low radar albedo.

The apparent depression of the instantaneous nighttime brightness temperatures (Fig. 3b) derived from the Galileo Orbiter's PPR data observed in the equatorial band is harder to explain than the radar analysis. Published models of increased surface roughness struggle to reproduce this effect<sup>4</sup>. However, we speculate that the reported reduction in instantaneous nighttime brightness temperatures may be a consequence of viewing angle effects. Because of the radiative scattering occurring within the penitentes, the tips of their blades cool significantly faster than the pits between them; oblique viewing angles will obstruct views of the pit interiors and so proportionately cooler temperatures would be presented to the observer.

Moreover, if anomalous circular polarization ratios on Europa observed in radar data are driven primarily by ordered surface roughness, similar polarization ratios on other icy moons of Jupiter<sup>18</sup> may indicate surfaces likewise roughened by penitente growth. We note that the Jovian system may occupy a restricted 'sweet spot' in the solar system for the development of such features formed in  $\text{H}_2\text{O}$  ice. Penitente formation is used to explain the extremely large ridges in the bladed terrain of Pluto, which are carved in massive deposits of methane ice<sup>19</sup>.

### Implications for future missions

In summary, we have performed an approximate calculation of sublimation rates on Europa, indicating that fields of penitentes may grow up to 15 m high in 50 Ma near the equator. We suggest that in equatorial regions sublimation erosion likely dominates over other erosional processes. Puzzling properties of the radar and thermal observations of Europa's equatorial belt can be explained by the presence of penitente fields in this region. The implications of penitente fields at potential landing sites should motivate further detailed quantitative analysis. Observations made by the upcoming Europa

Clipper mission high-resolution imaging system and ground-penetrating radar of these regions can directly test our conclusions.

## Online content

Any methods, additional references, Nature Research reporting summaries, source data, statements of data availability and associated accession codes are available at <https://doi.org/10.1038/s41561-018-0235-0>.

Received: 21 May 2018; Accepted: 24 August 2018;

Published online: 08 October 2018

## References

1. Greeley, R. et al. in *Jupiter: The Planet, Satellites and Magnetosphere* (eds Bagenal, F. & Dowling, T. E.) 329–362 (Cambridge University Press, Cambridge, 2004).
2. Luchitta, B. K. & Soderblom, L. A. in *Satellites of Jupiter* (ed. Morrison, D.) 521–555 (University of Arizona Press, Tucson, 1982).
3. Schenk, P. M., Matsuyama, I. & Nimmo, F. True polar wander on Europa from global-scale small-circle depressions. *Nature* **453**, 368–371 (2008).
4. Spencer, J. R., Tamppari, L. K., Martin, T. Z. & Travis, L. D. Temperatures on Europa from Galileo photopolarimeter-radiometer: nighttime thermal anomalies. *Science* **284**, 1514–1516 (1999).
5. Moore, J. M. et al. in *Europa* (eds Pappalardo, R. T. et al.) 329–349 (University of Arizona Press, Tucson, 2009).
6. Moore, J. M. et al. Mass movement and landform degradation on the icy Galilean satellites: results of the Galileo Nominal Mission. *Icarus* **140**, 294–312 (1999).
7. Buratti, B. J. & Golombek, M. P. Geologic implications of spectrophotometric measurements of Europa. *Icarus* **75**, 437–449 (1988).
8. Bierhaus, E. B., Zahnle, K. & Chapman, C. R. in *Europa* (eds Pappalardo, R. T., McKinnon, W. B. & Khurana, K. K.) 161–180 (University of Arizona Press, Tucson, 2009).
9. Johnson, R. E. et al. in *Europa* (eds Pappalardo, R. T., McKinnon, W. B. & Khurana, K. K.) 507–527 (University of Arizona Press, Tucson, 2009).
10. Domingue, D. L., Hapke, B. W., Lockwood, G. W. & Thompson, D. T. Europa's phase curve: implications for surface structure. *Icarus* **90**, 30–42 (1991).
11. Betterton, M. Theory of structure formation in snowfields motivated by penitentes, suncups, and dirt cones. *Phys. Rev. E* **63**, 056129 (2001).
12. Lliboutry, L. The origin of penitentes. *J. Glaciol.* **2**, 331–338 (1954).
13. Corripio, J. G. *Modelling the Energy Balance of High Altitude Glaciated Basins in the Central Andes* (Univ. Edinburgh, 2002).
14. Cathles, L. M. *Radiative Energy Transport on the Surface of an Ice Sheet* (Univ. Chicago, 2011).
15. Rhodes, J. J., Armstrong, R. L. & Warren, S. G. Mode of formation of 'ablation hollows' controlled by dirt content of snow. *J. Glaciol.* **33**, 135–139 (1987).
16. Claudin, P., Jarry, H., Vignoles, G., Plapp, M. & Andreotti, B. Physical processes causing the formation of penitentes. *Phys. Rev. E* **92**, 033015 (2015).
17. Ostro, S. J. et al. Europa, Ganymede, and Callisto: new radar results from Arecibo and Goldstone. *J. Geophys. Res.* **97**, 18227–18244 (1992).
18. Ostro, S. J. in *Satellites of Jupiter* (ed. Morrison, D.) 213–236 (Univ. Arizona Press, Tucson, 1982).
19. Moore, J. M. et al. Bladed terrain on Pluto: possible origins and evolution. *Icarus* **300**, 129–144 (2018).
20. Saur, J., Strobel, D. F. & Neubauer, F. M. Interaction of the Jovian magnetosphere with Europa: constraints on the neutral atmosphere. *J. Geophys. Res.* **103**, 19947–19962 (1998).
21. Moore, J. M. et al. Sublimation as a landform-shaping process on Pluto. *Icarus* **287**, 320–333 (2017).
22. Bergeron, V., Berger, C. & Betterton, M. Controlled irradiative formation of penitentes. *Phys. Rev. Lett.* **96**, 098502 (2006).
23. Cathles, L. M., Abbot, D. S. & MacAyeal, D. R. Intra-surface radiative transfer limits the geographic extent of snow penitentes on horizontal snowfields. *J. Glaciol.* **60**, 147–154 (2014).
24. Lhermitte, S., Abermann, J. & Kinnard, C. Albedo over rough snow and ice surfaces. *Cryosphere* **8**, 1069–1086 (2014).
25. Ward, W. R. & Canup, R. M. The obliquity of Jupiter. *Astrophys. J.* **640**, L91–L94 (2006).
26. Bierhaus, E. B. et al. Pwyll secondaries and other small craters on Europa. *Icarus* **153**, 264–276 (2001).
27. Paranicas, C., Cooper, J. F., Garrett, H. B., Johnson, R. E. & Sturmer, S. J. in *Europa* (eds Pappalardo, R. T., McKinnon, W. B. & Khurana, K. K.) 529–544 (Univ. Arizona Press, Tucson, 2009).
28. Morrison, D. & Morrison, N. in *Planetary Satellites* (ed. Burns, J.) 363–378 (Univ. Arizona Press, Tucson, 1977).
29. Grundy, W. M. et al. New horizons mapping of Europa and Ganymede. *Science* **318**, 234–237 (2007).
30. Schenk, P. M. Slope characteristics of Europa: constraints for landers and radar sounding. *Geophys. Res. Lett.* **36**, L15204 (2009).
31. Rathbun, J. A., Rodriguez, N. J. & Spencer, J. R. Galileo PPR observations of Europa: hotspot detection limits and surface thermal properties. *Icarus* **210**, 763–769 (2010).
32. Goldstein, R. M. & Green, R. R. Ganymede: radar surface characteristics. *Science* **207**, 179–180 (1980).
33. Ostro, S. J. & Pettengill, G. H. Icy craters on the galilean satellites? *Icarus* **34**, 268–279 (1978).
34. Campbell, B. A. High circular polarization ratios in radar scattering from geologic targets. *J. Geophys. Res.* **117**, E06008 (2012).

## Acknowledgements

We thank D. Blankenship, K. Mitchell, F. Nimmo and G. Tucker, and especially J. Spencer for discussions that shaped the form of this paper. Funding was from the Europa Pre-Project Mission Concept Study via the Jet Propulsion Laboratory, California Institute of Technology. We are grateful to P. Engebretson for contribution to figure production. We thank C. Chavez for her help with manuscript preparation.

## Author contributions

D.E.J.H. compiled data, performed and interpreted numerical analyses, and wrote the bulk of the paper. J.M.M. conceived and designed the study and organized the revision of the manuscript. A.D.H. was involved in the study, design, interpretation, and revision. Both J.M.M. and A.D.H. performed preliminary analyses. O.M.U. significantly revised the numerical analyses found in the Methods section. All authors discussed the results and commented on the manuscript.

## Competing interests

The authors declare no competing interests.

## Additional information

Reprints and permissions information is available at [www.nature.com/reprints](http://www.nature.com/reprints).

Correspondence and requests for materials should be addressed to D.E.J.H.

**Publisher's note:** Springer Nature remains neutral with regard to jurisdictional claims in published maps and institutional affiliations.

© The Author(s), under exclusive licence to Springer Nature Limited 2018

## Methods

We estimate a daily averaged amount of sublimated H<sub>2</sub>O ice from Europa based on following the methodology of Lebofsky<sup>35</sup>. We identify  $\rho_s q^{\text{avg}}$  to be the daily averaged mass loss rate of H<sub>2</sub>O ice (kg m<sup>-2</sup> s<sup>-1</sup>). The formula expressing this sublimation rate is given by

$$\begin{aligned} \rho_s q^{\text{avg}} &\approx \frac{\delta(T_{s0}) \cdot P_{\text{vap}}(T_{s0})}{4\pi v_a(T_{s0})} = \frac{P_{\text{vap}}(T_{s0})}{2\pi\sqrt{L}}; \\ v_a &\equiv \sqrt{\frac{kT_{s0}}{2\pi m_{H_2O}}}, \quad \delta(T_{s0}) \equiv \sqrt{\frac{2kT_{s0}}{\pi L m_{H_2O}}} \end{aligned} \quad (1)$$

The derivation of the above expression for  $\rho_s q^{\text{avg}}$  (see details below) takes into account the fact that most sublimation occurs in the few hours straddling high noon. The density of water ice is  $\rho_s = 920 \text{ kg m}^{-3}$ .  $P_{\text{vap}}$  is the temperature dependent vapour pressure of H<sub>2</sub>O.  $T_{s0}$  is the noon time temperature on Europa at a given latitude  $\lambda$ .  $\delta$  is a factor that is much less than one and accounts for the fact that most sublimation occurs around high noon. The characteristic velocity of particles in a Maxwell-Boltzmann gas is  $v_a$ . The Boltzmann constant is  $k$  and  $m_{H_2O}$  is the mass of a H<sub>2</sub>O molecule.  $L = 3 \times 10^6 \text{ J Kg}^{-1}$  is the heat of sublimation for H<sub>2</sub>O. The noon time temperature at a given latitude  $\lambda$  is estimated from the relationship

$$T_{s0} = \left[ \frac{(1-\omega)}{\sigma\epsilon} F_{\text{inc}} \right]^{1/4}; \quad F_{\text{inc}} = F_{\text{eur}} \cos\lambda, \quad F_{\text{eur}} \approx 50 \text{ W m}^{-2} \quad (2)$$

in which  $F_{\text{inc}}$  is the incident solar irradiance at latitude  $\lambda$ ,  $F_{\text{eur}}$  is the solar irradiance at Jupiter,  $\omega \sim 0.67$  is the surface albedo of Europa's ice and  $\epsilon \approx 0.9$  is its emissivity<sup>4,5,36</sup>. The Stefan-Boltzmann constant is  $\sigma$ . An analytic form for H<sub>2</sub>O's vapour pressure, which accounts for new experimental findings<sup>37</sup>, is discussed in detail below. Adopting an equatorial noon value of  $T_{s0} = 134 \text{ K}$ , we find that equation (1) predicts a sublimation lowering rate of about 0.3 m Ma<sup>-1</sup>, which amounts to 15 m of ice sublimated in 50 Ma which is the given average age of Europa's surface.

The remaining Methods section provides a detailed description of how we estimate the amount of ice sublimated away from Europa's surface. To lowest order we follow the methodology of Lebofsky<sup>35</sup> supplemented by the work of Cladoin et al.<sup>16</sup>. We define  $q$  to be the sublimation rate of surface ice (kg m<sup>-2</sup> s<sup>-1</sup>) divided by the surface ice density (kg m<sup>-3</sup>). Therefore  $q$  has units of m s<sup>-1</sup> and we write  $\partial_t h = q$ , where  $h$  is the level height of the ice. Three equations govern the evolution of  $h$  and the vapour content in Europa's ballistic atmosphere. The first of these represents the rate of change of  $h$  as driven by the balance of energy gained and lost,

$$\rho_s L \partial_t h = (1-\omega) F_{\text{inc}} - \epsilon \sigma T_s^4, \quad F_{\text{inc}} = F_{\text{jup}} \cos\lambda \quad (3)$$

where  $L = 3 \times 10^6 \text{ J kg}^{-1}$  is the heat of sublimation for H<sub>2</sub>O,  $F_{\text{inc}}$  is the incoming solar radiation at a given latitude on Europa's at noon where  $F_{\text{jup}} \sim 50 \text{ W m}^{-2}$  is the solar irradiance at Jupiter and  $\lambda$  is latitude.  $\omega \sim 0.67$  is the measured ice albedo for Europa's surface.  $\epsilon$  is the emissivity of Europa's surface ice. The surface ice density is  $\rho_s \sim 920 \text{ kg m}^{-3}$ . Finally,  $\sigma$  and  $T_s$  are respectively the Stefan-Boltzmann constant and the ice surface temperature. Note that  $T_s$  varies over the course of the day as the sun crosses the sky. The first expression on the right hand side of equation (3) represents the gain of solar irradiance while the second represents radiative losses to space. Note that for Europa, equation (3) is in very nearly steady state which means that to lowest order the expression is satisfied when  $(1-\omega)F_{\text{inc}} = \epsilon\sigma T_s^4$ . Based on analysis of brightness temperature data acquired by Galileo<sup>4,5</sup> as well as Voyager thermal emission spectra<sup>36</sup>, we adopt an emissivity  $\epsilon = 0.90$ . With peak brightness temperatures at equatorial noon to be about  $T_b \sim 131 \text{ K}$ , the above albedo and emissivity estimates yield a surface ice temperature at equatorial noon of  $T_s(t=\text{noon}) \equiv T_{s0} = T_b/\epsilon^{1/4} \approx 134.5 \text{ K}$ . We shall use assume this value to be typical of the equator at noon throughout.

The next equation follows the detailed change of the surface as a result of direct exchange between the atmosphere and vapour pressure driven sublimation,

$$\rho_s q = \rho_s \partial_t h = v_a (\rho_a - \rho_{\text{vap}}(T_s)); \quad v_a \equiv \left( \frac{kT_s}{2\pi m_{H_2O}} \right)^{1/2} \quad (4)$$

The quantity  $v_a$  is the typical value of the velocity in a Maxwell-Boltzmann distribution at temperature  $T_s$  and  $\rho_{\text{vap}}(T_s)$  is the saturation vapour density at  $T_s$ .  $m_{H_2O}$  is the mass of the hydrogen molecule.  $\rho_a$  is the surface mass density of water vapour. The equation represents the rate at which H<sub>2</sub>O molecules get absorbed by the surface (assuming 100% sticking probability) minus the rate the solid ice ablates due to its ice vapour pressure. Observations of Europa's noon time surface temperature<sup>4,5,9</sup> indicates a partial vapour pressure of H<sub>2</sub>O near its surface to be about a several 10<sup>-8</sup> Pa (see further below). With the relationship between vapour pressure and density given by  $\rho_{\text{vap}} = P_{\text{vap}}/c_s^2$ , where  $c_s \equiv \sqrt{kT/m_{H_2O}}$  is the isothermal sound speed, we find that the corresponding value for  $\rho_{\text{vap}}$  is approximately  $9.85 \times 10^{-13} \text{ kg m}^{-3}$ .

To illustrate the potential for penitente formation, we assume that all emitted water vapour is effectively lost which means setting  $\rho_a$  to zero, because Europa's atmosphere can be approximated as a vacuum. Thus, an upper bound estimate to the amount of surface H<sub>2</sub>O lost is given by

$$\rho_s \partial_t h = -v_a \rho_{\text{vap}}(T_s) = -P_{\text{vap}}(T_s) v_a / c_s^2 \quad (5)$$

Our task is to estimate a daily averaged value for  $v_a \rho_{\text{vap}}$ , which we hereafter refer to as  $\rho_s q^{\text{avg}}$ , and then extrapolate from this daily average to 50 Ma.

Because  $T_s$  varies over the course of the day and since  $P_{\text{vap}}$  has an Arrhenius form, calculating a daily average for the total number of H<sub>2</sub>O molecules emitted requires some finesse. However, an analytical form is possible. We designate  $t_{\text{day}}$  to be the length of one European day. We define the daily averaged vapour pressure to be

$$P_{\text{vap}}^{\text{avg}} \equiv \frac{1}{t_{\text{day}}} \int_{t_{\text{day}}} P_{\text{vap}}(T_s) dt, \quad (6)$$

For the vapour pressure of H<sub>2</sub>O, we fit a curve based on the data points acquired for water's phase diagram as summarized in Fray and Schmitt<sup>37</sup>. We note that the theoretical extrapolation of Feistel et al.<sup>38</sup> significantly underestimates H<sub>2</sub>O's vapour pressure compared to experimental findings for temperatures below  $T = 140 \text{ K}$ <sup>39,40</sup>, see also Fig. 3 of Fray and Schmitt<sup>37</sup>. We adopt the following fitted form to be a more accurate representation of H<sub>2</sub>O's behavior for the temperature range below 140 K:

$$\begin{aligned} P_{\text{vap}}(T) &\approx P_0 \exp \left[ \frac{L m_{H_2O}}{k} \left( \frac{1}{T_{130}} - \frac{1}{T} \right) \right]; \\ P_0 &= 2.30 \times 10^{-8} \text{ Pa}, \\ T_{130} &\equiv 130 \text{ K} \end{aligned} \quad (7)$$

$P_0$  is the measured value of H<sub>2</sub>O's vapour pressure at  $T = 130 \text{ K}$  based on a fit to the aforementioned experimental measurements<sup>39,40</sup>. We note that the previously estimated H<sub>2</sub>O sublimation rates on Europa<sup>9</sup>, which are based on the theoretical extrapolation of Feistel et al.<sup>38</sup>, are underestimated by a factor of six or more.

Given  $P_{\text{vap}}$ 's strong exponential dependence on  $1/T$ , over the course of one day the majority of surface sublimated H<sub>2</sub>O is emitted within a few hours around noon. Combining equation (3) with Europa's surface brightness temperature analysis<sup>4</sup>, the latter of which shows that Europa's surface temperature does not fall much below 74 K after the Sun sets, we adopt the following expression for Europa's surface temperature over the course of one European day:

$$\begin{aligned} T_s &= \max \left[ T_{s0} \left( \cos \frac{2\pi t}{t_{\text{day}}} \right)^{1/4}, T_{\min} \right]; \\ T_{s0} &\equiv \left[ \frac{(1-\omega) F_{\text{inc}}}{\sigma \epsilon} \right]^{1/4} \end{aligned} \quad (8)$$

where we have introduced  $T_{s0}$  to be the latitudinal dependent local noontime surface temperature. Because our concern is mostly centered on the few hours around noon, the surface temperature expression in equation (8) may be Taylor expanded as

$$T_s \approx T_{s0} \left[ 1 - \frac{1}{8} \left( \frac{2\pi t}{t_{\text{day}}} \right)^2 \right] \quad (9)$$

Inserting equation (9) into the daily averaged integral expression equation (6) via equation (7), and making use of well-known techniques in the asymptotic evaluation of integrals<sup>41</sup> we arrive at

$$\begin{aligned} P_{\text{vap}}^{\text{avg}} &= \delta(T_{s0}) \cdot P_{\text{vap}}(T_{s0}); \\ \delta(T_{s0}) &\equiv \sqrt{\frac{2kT_{s0}}{\pi L m_{H_2O}}} = \frac{2v_a}{\sqrt{L}} \end{aligned} \quad (10)$$

and the corresponding daily averaged flux of sublimated gas is given by the expression

$$\rho_s q^{\text{avg}} \approx \frac{P_{\text{vap}}^{\text{avg}}(T_{s0})}{4\pi v_a(T_{s0})} = \frac{\delta(T_{s0}) \cdot P_{\text{vap}}(T_{s0})}{4\pi v_a(T_{s0})} = \frac{P_{\text{vap}}(T_{s0})}{2\pi \sqrt{L}} \quad (11)$$

Equation (10) says that the daily averaged vapour pressure is equal to the vapour pressure at noon diminished by the multiplicative factor  $\delta$ , while equation (11) gives the corresponding daily averaged sublimated mass-flux of H<sub>2</sub>O from the surface.

For example, for a surface temperature at the equator in which  $T_{s0} = 134$  K, we find that  $v_o \approx 98.5$  m s $^{-1}$  and that  $\delta = 0.114$ . Based on equation (7),  $P_{vap}(T_{s0}) \approx 1.02 \times 10^{-7}$  Pa. Thus, the daily averaged mass flux of H<sub>2</sub>O at the equator is approximately  $\rho_o q^{avg} = 9.37 \times 10^{-12}$  kg m $^{-2}$  s $^{-1}$ , which is equivalent to  $3.13 \times 10^{10}$  H<sub>2</sub>O molecules cm $^{-2}$  s $^{-1}$ —a figure that is 6–9 times larger than previous estimates<sup>42,43</sup>. This loss rate translates to approximately  $2.98 \times 10^3$  Kg m $^{-2}$  Ma $^{-1}$ , which is equivalent to about 15 m of ice over 50 Ma.

## Data availability

The data that support the findings of this study are available on the NASA Planetary Data System (PDS) (<https://pds.nasa.gov/>).

## References

35. Lebofsky, L. A. Stability of frosts in the solar system. *Icarus* **25**, 205–217 (1975).
36. Spencer, J. R. *The Surfaces of Europa, Ganymede, and Callisto: An Investigation Using Voyager IRIS Thermal Infrared Spectra* (Univ. Arizona, 1987).
37. Fray, N. & Schmitt, B. Sublimation of ices of astrophysical interest: a bibliographic review. *Planet. Space. Sci.* **57**, 2053–2080 (2009).
38. Feistel, R. & Wagner, W. Sublimation pressure and sublimation enthalpy of H<sub>2</sub>O ice Ih between 0 and 273.16 K. *Geochim. Cosmochim. Acta* **71**, 36–45 (2007).
39. White, B. E., Hessinger, J. & Pohl, R. O. Annealing and sublimation of noble gas and water ice films. *J. Low Temp. Phys.* **111**, 233–246 (1998).
40. Mauersberger, K. & Krankowsky, D. Vapor pressure above ice at temperatures below 170 K. *Geophys. Res. Lett.* **30**, 1121 (2003).
41. Bender, C. M. & Orszag, S. A. *Advanced Mathematical Methods for Scientists and Engineers* (McGraw-Hill, New York, 1978).
42. Shematovich, V. I., Johnson, R. E., Cooper, J. F. & Wong, M. C. Surface bound atmosphere of Europa. *Icarus* **173**, 480–498 (2005).
43. Smyth, W. H. & Marconi, M. L. Europa's atmosphere, gas tori, and magnetospheric implications. *Icarus* **181**, 510–526 (2006).